Corrections to Landau Fermi-liquid fixed-point approximation in nonlinear bosonized theory: An application to g_A^L in nuclei

Long-Qi Shao [1,2,3,*] and Mannque Rho [4,†]

[1] *School of Fundamental Physics and Mathematical Sciences, Hangzhou Institute for Advanced Study, UCAS, Hangzhou 310024, China*

[2] *Institute of Theoretical Physics, Chinese Academy of Sciences, Beijing 100190, China*

[3] *University of Chinese Academy of Sciences, Beijing 100049, China*

[4] *Université Paris-Saclay, CNRS, CEA, Institut de Physique Théorique, 91191, Gif-sur-Yvette, France*

(Received 1 March 2024; accepted 21 June 2024; published 11 July 2024)

We calculated in nonlinear bosonized theory $1/\bar{N}$ corrections to the Landau Fermi-liquid fixed-point (FLFP) axial-vector coupling constant in nuclear matter $g_A^L \approx 1$ to which the Landau parameter F_1^ω predominantly contributes. We obtain the correction to F_1^ω to calculate the correction δg_A^L to the axial-vector coupling constant g_A^L at the nuclear saturation density. It comes out to be extremely small, $\delta g_A^L \sim O(10^{-4})$. We discuss how the dilaton-limit fixed-point (DLFP) result $g_A = 1$ can be preserved from finite nuclei to high densities relevant to massive neutron stars and its possible impact on $0\nu\beta\beta$ decay processes involved in going beyond the standard model.

DOI: 10.1103/PhysRevC.110.015204

I. INTRODUCTION

It has been argued [1] that when a many-nucleon system is treated as interacting fermions in renormalization-group approach on the Fermi surface, the superallowed Gamow-Teller transition (with momentum transfer $q \approx 0$) is described by the Fermi-liquid fixed-point coupling constant g_A^L captured entirely by the strong nuclear correlation effects of the quasiparticle on the surface. This meant that the longstanding puzzle of the quenched $g_A^* \approx 1$ observed in light nuclei [2,3] can be accounted for in terms of a quasiparticle effective axial-vector coupling constant in nuclear effective field theory (EFT) defined by the chiral cutoff scale $\approx 4\pi f_\pi \approx 1$ GeV

$$g_A^* = g_A^L \approx 1. \tag{1}$$

This result should apply to not just light nuclei but also to heavy nuclei and perhaps all the way to massive compact star matter. How this result could impact on nuclear dynamics in general and the search for going beyond the standard model will be commented on in Sec. III.

Up to date there is no *ab initio* microscopic many-body calculation to confirm or dismiss the prediction (1). Highly powerful Monte Carlo calculations [4] that have been performed for light nuclei with mass number $A \leqslant 21$ indicate no hint for such a renormalized coupling constant g_A^* in many nucleon systems. Modulo possibly small corrections from n-body (for $n \geqslant 2$) current operators, what could be referred to as fundamental $g_A = 1.276$ can fully account for the axial transitions in nuclear medium. But there is no such fully trustful microscopic calculation available up to date for heavier nuclei.

The aim of this paper is to show that the prediction (1) remains to hold unaffected at least up to $\lesssim; n_0$ (where $n_0 \approx 0.16$ fm^{-3} is the normal nuclear matter density) under corrections to the Fermi-liquid fixed-point approximation that gave (1). The strategy we use is to apply to nuclear interactions the technique of nonlinear bosonization of Fermi surfaces anchored on the method of coadjoint orbits developed in condensed matter physics [5]. For the strong interactions involved, we need to implement the degrees of freedom associated with QCD, endowed with both intrinsic and hidden symmetries, which bring to the problem complexities absent in, and different from, condensed matter systems.

The calculation involved consists of three elements. The first is the notion that the theory for strong interactions, QCD, gives the nucleons, i.e., light-quark baryons, as the skyrmions—and equivalently the weakly interacting constituent quarks—in the limit of large number of colors $N_c \to \infty$. Embedded in a skyrmion medium, the effective quasiskyrmion mass that we could refer to as chiral quasiparticle mass scales in density as [6][1]

$$m_N^{\text{skyrmion}*}/m_N \approx (g_A^*/g_A)^{1/2} f_\pi^*/f_\pi. \tag{2}$$

Here and in what follows, $*$ stands for density dependence. What is taken into account in (2) is, apart from the large N_c

*Contact author: shaolongqi22@mails.ucas.ac.cn

†Contact author: mannque.rho@ipht.fr

[1] In this reference, $f_\chi^*/f_\chi \approx f_\pi^*/f_\pi$ and the latter is given experimentally in deeply bound pionic atom. This relation most likely does not hold in other cases, e.g., for dilatonic Higgs models for large N_f [7].

limit, scale invariance of the axial coupling to skyrmions at the classical level and the in-medium dilaton σ_d condensate $\langle\sigma_d\rangle \propto \langle\chi\rangle$ where χ here is the linearly scale-transforming conformal compensator field $\chi = f_\chi e^{\sigma_d/f_\chi}$ figuring in the effective field theory Lagrangian. In (2) f_π^*/f_π replaces f_χ^*/f_χ as explained later. One can identify (2) as an in-medium Goldberger-Treiman relation. It is established that in the vacuum, the Goldberger-Treiman relation holds very well in the large N_c limit and we assume that it will also do so in medium.

The next thing we want to establish is the connection between the chiral effective field theory for nuclear matter and the effective field theory for Landau Fermi liquid of nucleons. Extending effective field theory on the Fermi surfaces developed for condensed matter systems [8,9] to nuclear chiral effective field theory incorporating hidden (both vector and scalar) symmetries for strongly interacting nuclear systems [10], it has been shown that

$$m_L^*/m_N \approx (1-\tilde{F}_1/3)^{-1}, \tag{3}$$

where m_L^* is the Landau (fixed-point) quasiparticle (a.k.a. nucleon) mass and

$$\tilde{F}_1 = (m_N/m_L^*)F_1 \tag{4}$$

with

$$F_1 = F_1^\omega + F_1^\pi, \tag{5}$$

where $F_1^{\omega(\pi)}$ stands for the contribution from the Landau quasiparticle interaction in the $\omega(\pi)$ channel. What makes the nuclear Fermi-liquid system strikingly different from the electron Fermi liquid is the Landau quasiparticle interaction in the pion channel F_1^π, which will turn out as we will elaborate below to play a crucial role in nuclear properties.

Third, the basic premise of our theory is that the chiral mass (2) valid at the large N_c limit can be equated to the Landau mass (3) in the Fermi-liquid fixed-point approximation

$$m_N^{\text{skyrmion}*}/m_N \approx m_L^*/m_N. \tag{6}$$

It follows from (2) that

$$g_A^* \approx g_A\left(1-\frac{1}{3}\Phi_\chi^*\tilde{F}_1^\pi\right)^{-2}, \tag{7}$$

where

$$\Phi_\chi^* = f_\chi^*/f_\chi \approx f_\pi^*/f_\pi \tag{8}$$

with the last approximate equality assumed to hold in the genuine dilaton (GD) model [11,12].

It will be our assertion that one can take the quasiskyrmion g_A^* to be equivalent to the Landau fixed-point quantity g_A^L

$$g_A^L \approx g_A\left(1-\frac{1}{3}\Phi_\chi^*\tilde{F}_1^\pi\right)^{-2}. \tag{9}$$

It turns out that the product $\frac{1}{3}\Phi_\chi^*\tilde{F}_1^\pi$ is more or less independent of density near n_0, so one arrives at

$$g_A^L \approx 1 \tag{10}$$

that applies not only to light nuclei but also to nuclear matter at a density $\sim n_0$. What will be surprising is that $g_A^L \to 1$ exactly at what is called dilaton-limit fixed-point (DLFP) [13] at some high density near chiral restoration.

What takes place in between is the main topic of this paper. It will be found that the higher-order corrections found in the framework adopted in this paper to Eq. (10) are extremely small, $\sim O(10^{-4})$, even at the normal nuclear matter density n_0. What this result, if correct, implies both in the superallowed Gamow-Teller transitions in nuclei as well as in the $0\nu\beta\beta$ transitions relevant for going beyond the standard model will be discussed in Sec. III.

II. GENERALIZED CHIRAL EFFECTIVE FIELD THEORY: G*n*EFT

Our approach is anchored on an effective Lagrangian that incorporates hidden local symmetry (HLS) [14,15] and hidden scale symmetry (HSS) [11] into chiral EFT mapped to Fermi liquid applicable to nuclear matter (in place of electron systems). Hidden local symmetry comprising the lightest vector mesons ρ and ω is gauge equivalent to nonlinear σ model [14] so can be simply implemented at the classical level [that is at the leading-order chiral power counting, $O(p^2)$, in the mesonic sector and $O(p)$ when baryons are coupled]. Hidden scale symmetry is implemented using the conformal compensator field χ with a suitable dilaton potential V_d appropriate for the GD scale symmetry. For the problem we are concerned with we do not need to enter the detailed structure given in the reviews [16,17]. The formulation made in these reviews involves the mechanism for hadron-quark continuity at a density above n_0, typically $\approx 3n_0$, to access the density relevant to the interior of massive compact stars. Although the precise way the crossover from hadrons to quarks/gluons takes place may not matter quantitatively in the properties of compact stars, for the problem concerned here at near nuclear matter density, what turns out to be most relevant is the intricate interplay between the coupling of the pions, the ω and σ_d to nucleons. This aspect of the problem has not yet been treated in the literature.

A. Interplay between ω meson coupling and σ_d meson coupling

In arriving at Eq. (7), what is involved is an interplay between the ω and σ_d mesons in nuclear matter treated as a Fermi liquid on the Fermi surface. For this matter, what is most important is the notion of the genuine dilaton (GD for short) in QCD as put forward by Crewther and collaborators [11,12]. The GD scheme is characterized by the assumption that there exists an infrared fixed point (IRFP) α_{IR} for $N_f \leqslant 3$ at which both scale symmetry and chiral symmetry (in the chiral limit) are realized in the Nambu-Goldstone (NG) mode, populated by the massless NG bosons π and dilaton σ_d whose decay constants are nonzero. The characteristic of this notion that we espouse is that it accommodates the massive nucleons Ψ and vector mesons $V_\mu = (\rho, \omega)$ at the IR fixed point.

The GD in a chiral Lagrangian plays not only the role of reducing the nucleon mass from m_N to m_N^σ by the attractive coupling to a scalar σ in Walecka mean-field theory [18] but also endows the BR scaling [6] caused by the vacuum change

by nuclear medium

$$\frac{m_V^*}{m_V} \approx \frac{m_s^*}{m_s} \approx \frac{f_\pi^*}{f_\pi} \equiv \Phi_\chi^*, \tag{11}$$

where V means vector meson, m_V the vector meson mass, m_s the scalar (either Walecka's σ or σ_d in GnEFT) meson mass.

In mapping to Fermi liquid, we integrate out the ω and π mesons, leaving local four-fermion and nonlocal four-fermion interactions, respectively (ρ channel will not figure in the calculation of g_A^L, but will figure in the calculation of the gyromagnetic ratio mentioned below). The quasiparticle energy is

$$\varepsilon(p) = \frac{p^2}{2m_N^\sigma} + C_\omega^2 n + \Sigma_\pi(p), \tag{12}$$

where m_N^σ is the BR-scaled nucleon mass and $C_\omega^2 = g_\omega^2/m_\omega^{*2}$ with g_ω the ω-N coupling constant. $\Sigma_\pi(p)$ is self-energy given by the pionic Fock term. Taking derivatives with respect to momentum at the Fermi surface

$$\left.\frac{d\varepsilon(p)}{dp}\right|_{p=p_F} = \frac{p_F}{m_L^*} = \frac{p_F}{m_N^\sigma} + \left.\frac{d\Sigma_\pi(p)}{dp}\right|_{p=p_F}, \tag{13}$$

where p_F is the Fermi momentum. Equation (2), Eq. (3), Eq. (6), and the Fock term at n_0 [19]

$$\tilde{F}_1^\pi = -3\frac{m_N}{p_F}\left.\frac{d\Sigma_\pi(p)}{dp}\right|_{p=p_F} \tag{14}$$

lead us to identify $g_A^L \approx 1$, Eq. (9), as a Landau fixed point quantity. A quantity that figures importantly to justify this is the relation

$$\frac{m_N}{m_N^\sigma} = \Phi_\chi^{*-1} = 1 - \frac{1}{3}\tilde{F}_1^\omega. \tag{15}$$

The quantities involved here are taken to be Landau fixed-point (LFP) quantities. What we will calculate below as $1/\bar{N}$ corrections deal with the LFP quantities and the relation (15) correlates the attractive interaction effect associated with the dilaton, i.e., the BR scaling, and the repulsion due to ω exchange. Although we have not fully understood—a task we have left for the future work, we think it is this relation that dictates intricately the size of the $1/\bar{N}$ corrections estimated in this paper.

B. Mesonic fields

As stated, in formulating renormalization group approaches to interacting nucleons, it is more astute to introduce mesonic fields *ab initio* that are massive such as the light-quark vector mesons (ρ, ω) in addition to the pseudo-Nambu-Goldstone bosons π, σ_d, etc. For very low-energy excitations or densities, the bosonic fields can be integrated out with higher derivative terms appearing. In fact even the pions can be integrated out leading to pionless EFT, which can be treated in terms of the power series. The pionless EFT will breakdown if the excitation involves the scale higher than the pion mass. The standard chiral EFT (SχEFT) anchored on the chiral Lagrangian with nucleons and pions has been shown to work well up to the scale corresponding to the scale of the masses of the mesons integrated out, say $O(m_\rho)$. The power expansion goes typically to N^{q}LO for $q \leqslant 3$ and is to breakdown when the scale involved goes above m_ρ. The SχEFT therefore is expected not to work for compact-star densities where the density involved is $\approx$(4–7)n_0.

The approach mentioned in the previous section that maps GnEFT Lagrangian to the Landau Fermi-liquid fixed-point theory of many-nucleon systems can circumvent such difficulty. When the nucleons are put on the Fermi surface, the Fermi-liquid fixed-point (FLFP) approximation corresponds to taking $1/\bar{N}$ to zero, where $\bar{N} = p_F/\Lambda$ with Λ the cutoff with respect to the Fermi surface. It becomes more reliable as density increases. When we consider Λ to be a finite quantity small compared to p_F, the $1/\bar{N}$ correction should enter into the fixed-point result Eq. (1). This is the double-decimation procedure applied in $V_{\text{low k}}$ RG in finite nuclei [20]. The main result of this paper is that Eq. (1) still holds when $1/\bar{N}$ correction enters.

Before going into the $1/\bar{N}$ corrections, it should be noted that the pion and ω contribute differently to the FLFP result. To illustrate this, we explain how the gyromagnetic ratio for the proton in heavy nuclei g_l^p comes out in the FLFP approximation in GnEFT. The calculation is essentially the same as the simplified chiral Lagrangian with HLS fields implemented with the hidden scale symmetry used in Ref. [21]. We will therefore simplify the discussion, leaving the details to Ref. [21].

In GnEFT, the Lagrangian taken at the mean-field (viz, FLFP) approximation [8,10] gives the Migdal formula [22] for the quasiparticle convection current

$$\boldsymbol{J} = \frac{\boldsymbol{p}}{m_N} g_l = \frac{\boldsymbol{p}}{m_N}\left(\frac{1+\tau_3}{2} + \frac{1}{6}(\tilde{F}_1 - \tilde{F}_1')\tau_3\right), \tag{16}$$

where $\tilde{F}_1 = \tilde{F}_1^\pi + \tilde{F}_1^\omega$, $\tilde{F}_1' = \tilde{F}_1'^\pi + \tilde{F}_1'^\rho$, and $g_l = (1+\tau_3)/2 + \delta g_l$, where δg_l is the anomalous gyromagnetic ratio $\delta g_l = \delta g_l^0 + \delta g_l^1$ with (0,1) standing for (isoscalar, isovector). It was found [10] that

$$\delta g_l^0 = 0, \tag{17}$$

$$\delta g_l^1 = \frac{4}{9}\left[\Phi_\chi^{*-1} - 1 - \frac{1}{2}\tilde{F}_1^\pi\right]\tau_3. \tag{18}$$

It turns out that the prediction (18) agrees precisely with the available experiment [23].

Now going from the EFT chiral Lagrangian to the Migdal formula is highly nontrivial, the details of which are found in Refs. [10,21]. The intricacy comes in two ways. First, the nucleon mass that figures in the Lagrangian is the BR scaled mass m_N^σ, so the single-nucleon convection current will be $\boldsymbol{J}_{\text{1-body}} = \frac{\boldsymbol{p}}{m_N^\sigma}\frac{1+\tau_3}{2}$. As explained in Ref. [21], this would violate the $U_{\text{EM}}(1)$ gauge invariance. Second, the same holds when m_N^σ is replaced by the Landau mass m_L^*. This problem known in condensed matter systems as Kohn effect can be remedied when two-body exchange currents involving the vector meson exchange currents are taken into account [21]. What figures there is what is known as back-flow current that is required by Ward identity. It effectively restores the $U(1)$ gauge invariance. This means that whatever figures as

corrections in F_1^ω should be constrained by the gauge invariance involving Ward identity.

Now the $U(1)$ gauge invariance says nothing about the isovector part, Eq. (18), so there is no such constraint in the ρ channel. However, in deriving Eq. (18), the nonet relation $C_\rho^2 = C_\omega^2/9$ was used, so the ρ channel contributes in the same way as ω channel except for the coupling constant and the isospin matrix; so we have $\tilde{F}_1^{\prime\rho} = \tilde{F}_1^\omega/9$, which also holds when $1/\bar{N}$ corrections are included. The contribution of the ρ channel in Eq. (18) was represented by Φ_χ^* through Eq. (15). The fact that Eq. (18) agrees well with experiments tells us that the corrections to $\tilde{F}_1^\pi$ and $\tilde{F}_1^{\prime\rho}$ should cancel each other significantly or both be small, otherwise the good result Eq. (18) will be spoiled. The above theory based on the chiral Lagrangian implemented with hidden local and scale symmetries in the FLFP approximation gives satisfying results for g_A^L and δg_l^p. The renormalizations of the vertices involved are in one-to-one correspondence with the nucleon self-energy except for the isospin index. Given that the $\tilde{F}_1^{\prime\rho}$ is closely related to F_1^ω, whose correction turn out to be small, we will assume the possible corrections to F_1^π are ignorable, i.e., corrections to $\tilde{F}_1^\pi$ and $\tilde{F}_1^{\prime\rho}$ are both small to preserve the good result for gyromagnetic ratio.

What is important in our problem concerned here is the ω meson contribution to the BR-scaled nucleon mass (15). At the mean-field level (that is, in the FLFP approximation), it is connected to the universal BR scaling Φ_χ^*. However, if one goes beyond the FLFP approximation—that is higher order in $1/\bar{N}$–$\tilde{F}_1^\omega$ will be modified and as a consequence, the nucleon mass will scale differently from the universal BR scaling $\Phi_\chi^* = f_\pi^*/f_\pi$.

We denote the modification as the nucleon mass shift associated with the ω exchange

$$m_N^\sigma \to m_N^\sigma + \delta m_N^\omega. \tag{19}$$

It is important to note that this modified scaling should not affect the $U(1)$ gauge invariance.

C. $1/\bar{N}$ corrections

Now let us return to the g_A problem (9). We would like to see how $g_A^L \approx 1$ is modified by corrections to the FLFP approximation and also by the increase of density beyond the normal matter density n_0. Let us mention that the g_A^L at higher density is not an academic curiosity. In fact, as already mentioned, it is closely linked to the possible property of the GD at what is termed DLFP at the density at which $\langle\chi\rangle$ goes to zero [13]. It is also connected to the possible precocious onset of the pseudoconformal sound speed [17]. What is at issue in the behavior of g_A^L is the product of the two quantities $\tilde{F}_1^\pi$ and Φ_χ^*, which also figure in the convection current discussed above. The question then is how these quantities are modified by the corrections.

We first consider $\tilde{F}_1^\omega$. From Eq. (15)

$$\frac{m_N}{m_N^\sigma} = 1 - \frac{1}{3}\tilde{F}_1^\omega. \tag{20}$$

We see that the scaling of the nucleon mass by the BR scaling capturing the role of the attraction brought by the dilaton field is tied to the property of the ω contribution to the Landau parameter. At the Fermi-liquid fixed point, it is given by the universal BR scaling factor Φ_χ. Going beyond the FLFP approximation, it will depend on the vector meson (ρ or ω) exchanged. Here it will be the ω channel whereas in δg_l^1, Eq. (18), it will be the ρ channel. In principle they could be different.

Now we focus on calculating δm_N^ω in Eq. (19). For this we need the standard textbook notations for Landau-Fermi-liquid theory applied to nuclear systems. The variation of the energy of the system is given by

$$\delta E = \sum_{\boldsymbol{p}} \varepsilon_p \delta f(\boldsymbol{p}) + \frac{1}{2V}\sum_{\boldsymbol{p},\boldsymbol{p}'} \mathcal{F}(\boldsymbol{p},\boldsymbol{p}')\delta f(\boldsymbol{p})\delta f(\boldsymbol{p}'), \tag{21}$$

where ε_p is the quasiparticle energy, $\delta f(\boldsymbol{p})$ is the deviation of the fermion occupation number from the ground state, V is the volume, $\mathcal{F}(\boldsymbol{p},\boldsymbol{p}')$ are quasiparticle interactions on the Fermi surface,

$$\begin{aligned}\mathcal{F}(\boldsymbol{p},\boldsymbol{p}') = f(\cos\theta) + f'(\cos\theta)(\boldsymbol{\tau}\cdot\boldsymbol{\tau}') + g(\cos\theta)(\boldsymbol{\sigma}\cdot\boldsymbol{\sigma}') \\ + g'(\cos\theta)(\boldsymbol{\tau}\cdot\boldsymbol{\tau}')(\boldsymbol{\sigma}\cdot\boldsymbol{\sigma}')\end{aligned} \tag{22}$$

with

$$f(\cos\theta) = \sum_{l=0}^{\infty} f_l P_l(\cos\theta),\ \ f'(\cos\theta) = \sum_{l=0}^{\infty} f_l' P_l(\cos\theta), \tag{23}$$

where $P_l(\cos\theta)$ are Legendre polynomials. The dimensionless Landau parameters we use are

$$F_l = N f_l,\ \ F_l' = N f_l', \tag{24}$$

where N is the fermion density at the Fermi surface

$$N = \frac{\nu m_L^* p_F}{2\pi^2}, \tag{25}$$

where ν is degeneracy factor, and m_L^* the Landau effective mass.

1. Fermi-liquid fixed-point approximation

We first calculate F_1^ω in the Landau Fermi-liquid fixed-point approximation. This can be done by first reducing the G*n*EFT Lagrangian to Walecka's linear σ/ω model [18,24]

$$\begin{aligned}\mathcal{L} = \bar{\Psi}(i\partial\!\!\!/ - m_N)\Psi + \frac{1}{2}\left(\partial_\mu\sigma\partial^\mu\sigma - m_s^2\sigma^2\right) \\ - \frac{1}{2}\left(\frac{1}{2}\omega_{\mu\nu}\omega^{\mu\nu} - m_\omega^{*2}\omega_\mu\omega^\mu\right) \\ + g_s\bar{\Psi}\Psi\sigma - g_\omega\bar{\Psi}\gamma_\mu\Psi\omega^\mu\end{aligned} \tag{26}$$

and then doing relativistic mean-field calculation. It corresponds to taking one-loop term in Fig. 1.

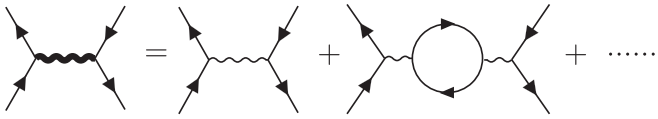

FIG. 1. Two-body interactions by ω exchange; the thick wavy line represents the full ω propagator, the thin wavy line the free ω meson propagator, the solid line the nucleon with Walecka effective mass m_N^σ.

From Fig. 1 one can write down the two-body nuclear interaction as

$$f^\omega(\boldsymbol{p},\boldsymbol{p'}) = \bar{u}(p)\gamma^\mu u(p) D_\omega \bar{u}(p')\gamma_\mu u(p') + \bar{u}(p)\gamma^\mu u(p) D_\omega \Pi_{\mu\nu} D_\omega \bar{u}(p')\gamma^\nu u(p') + \cdots, \tag{27}$$

where D_ω is the free ω meson propagator

$$D_\omega = \frac{g_\omega^2}{m_\omega^{*2} - q_\mu q^\mu} \tag{28}$$

and $\Pi_{\mu\nu}$ is the polarization tensor of ω meson field. Taking in the polarization tensor $\Pi_{\mu\nu}$ the forward scattering limit $|\boldsymbol{q}|/q_0 \to 0$ one finds that only the Π_{ii} component is nonvanishing

$$\Pi_{ii} \approx \frac{n}{E_F}, \tag{29}$$

where $E_F = \sqrt{m_N^{\sigma 2} + p_F^2}$ and n is the nuclear matter density. We equated the shifted scalar mass in the mean-field calculation to the BR-scaled nucleon mass. Using Eq. (28), Eq. (29), and the spinor u, we get F_1^ω [with the Legendre polynomial $P_1(\cos\theta) = \cos\theta$],

$$\frac{1}{3}F_1^\omega = \frac{1}{3} f_1 \cdot N = -\frac{1}{3} C_\omega^2 \frac{p_F^2}{E_F^2\left(1 + C_\omega^2 \Pi_{ii}\right)} \cdot \frac{\nu p_F m_L^*}{2\pi^2}. \tag{30}$$

We see that it is the polarization tensor Π_{ii} that controls F_1^ω. To reproduce the FLFP result in Ref. [10], we resort to the nonrelativistic form

$$\Pi_{ii} = \frac{n}{m_N^\sigma}, \quad \frac{1}{3}F_1^\omega = -C_\omega^2 \frac{n m_L^*}{m_N^\sigma\left(m_N^\sigma + C_\omega^2 \Pi_{ii} m_N^\sigma\right)}. \tag{31}$$

2. To go beyond the FLFP approximation

It is possible to go beyond the FLFP approximation by using the $V_{\text{low k}}$ renormalization-group approach [20]. A brief remark will be given below regarding this approach. We find a more systematic and possibly more powerful method is to to apply the nonlinear bosonized theory (NBT) [5]. We will first reproduce the polarization tensor in Eq. (31) using the NBT and then calculate the corrections to the polarization tensor denoted $\delta\Pi_{ii}$.

The nonlinear bosonized theory uses bilinear fermion operators as exponential of bosonic degrees of freedom, which can be seen as particle-hole excitations on the Fermi surface. The Lagrangian is

$$S = \int dt \langle f_0, U^{-1}(\partial_t - \varepsilon)U\rangle, \tag{32}$$

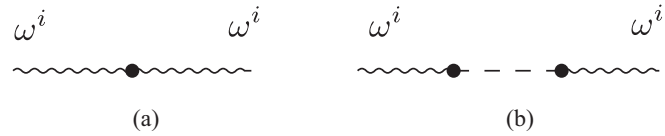

FIG. 2. The leading-order corrections to the free ω propagator, the dashed line represents the bosonic field ϕ, the wavy line the spatial component of the ω meson. The black dots represent different vertices in the Lagrangian.

where $f_0(\boldsymbol{p}) = \Theta(|\boldsymbol{p}| - p_F)$ is the ground-state fermion occupation number and $U = \exp(-\phi)$ with ϕ the dynamical bosonic degree of freedom that characterizes nonlinear structure of Fermi surface, ϕ lives on both momentum space and coordinate space.

$$\int dt \langle A, B\rangle = \int dt d\boldsymbol{x} d\boldsymbol{p} A \cdot B, \tag{33}$$

$$U^{-1}AU = A + \{\phi, A\} + \frac{1}{2!}\{\phi, \{\phi, A\}\} + \cdots, \tag{34}$$

where $\{,\}$ is the Poisson bracket.

The first term in Eq. (32) is the Wess-Zumino-Witten (WZW) term that captures the geometric phase when the Fermi surface evolves with time, while the second term is the normal quasiparticle energy term. For convenience, we use the nonrelativistic $\varepsilon = p^2/2m_N$.

As in Sec. II, we incorporate σ and ω fields, use Walecka's mean-field approximation by integrating out the σ meson and change $m_N \to m_N^\sigma$ (which can be considered as the BR-scaled mass)

$$S = \int dt \left\langle f_0, U^{-1}\left(\partial_t - \omega_0 - \frac{(\boldsymbol{p} + \boldsymbol{\omega})^2}{2m_N^\sigma}\right)U\right\rangle + S_\omega, \tag{35}$$

where S_ω is the ω meson sector, ω_0 and $\boldsymbol{\omega}$ are the four-component ω_μ.

With U expanded in different orders in ϕ, we can calculate the ω propagators systematically. The details of the power counting and calculations are given in the Appendix. The leading-order corrections to the free ω propagators are shown in Fig. 2.

As in the fermion description, we are interested in Π_{ii}, so only the spatial components of the ω meson are involved. The leading-order corrections, the details of which are relegated to Appendix B, are

$$\Pi_{ii} = -\frac{\nu p_F^3}{6\pi^2 m_N^\sigma} \frac{m_N^\sigma |q_0|}{2p_F|\boldsymbol{q}|} \log \frac{m_N^\sigma |q_0| - p_F|\boldsymbol{q}|}{m_N^\sigma |q_0| + p_F|\boldsymbol{q}|}. \tag{36}$$

In the limit $|\boldsymbol{q}|/q_0 \to 0$, $\Pi_{ii} = n/m_N^\sigma$, the same as Eq. (31).

The next-order diagrams are $1/\tilde{N} = \Lambda/p_F$ suppressed. There are more diagrams at this order. However, it turns out that in the limit $q_0 \to 0$, $|\boldsymbol{q}| \to 0$ and $|\boldsymbol{q}|/q_0 \to 0$, only one diagram Fig. 3 survives.

Notice that the nonlinear structure has not yet entered in the diagrams we have dealt with so far. The reason is that no vertices that connect two dashed lines appear in these diagrams. Such vertices will appear at higher orders or if we

FIG. 3. Next-order corrections to the free ω meson propagator.

loosen the constraint that q_0 and $|\boldsymbol{q}|$ approach zero in the way $|\boldsymbol{q}|/q_0 \to 0$ as shown in Fig. 4.

The calculation of Fig. 3 involves large momentum transfer [8] as presented in Appendix B 2. We will designate this diagram as $1/\bar{N}$ correction to the ω meson propagator and also to F_1^ω. The result is (see Appendix B)

$$\delta\Pi_{ii} = -\frac{\nu\Lambda g_\omega^2}{64\pi^4 m_N^{\sigma 2}} \int_\Lambda^{2p_F} dk \frac{k^4}{k^2 + m_\omega^{*2} - \frac{k^2\sqrt{k^2+m_\omega^{*2}}}{2m_N^\sigma}}. \quad (37)$$

We have assumed that the ω-meson-exchange Landau parameter F_1^ω and the pion exchange F_1^π are not correlated at the order considered as at the FLFP limit [10]. Since we are near the FLFP, we consider this to be reasonable.

3. $1/\bar{N}$ correction to g_A^L

We have derived the $1/\bar{N}$ corrections to the ω propagators in Sec. II C 2. The corrections to the ω meson propagators will directly modify the F_1^ω induced by the exchange of the ω meson. According to the argument made in Sec. II A, Eq. (15) is essential for preserving gauge invariance. We propose as in Eq. (19) that since Eq. (12) corresponds to the FLFP result, when we are away from the FLFP, m_N^σ should be replaced by $m_N^\sigma + \delta m_N^\omega$. We define

$$\zeta = \frac{m_N^\sigma + \delta m_N^\omega}{m_N}. \quad (38)$$

The quasiparticle energy becomes

$$\varepsilon(p) = \frac{p^2}{2\left(m_N^\sigma + \delta m_N^\omega\right)} + C_\omega^2 n + \Sigma_\pi(p). \quad (39)$$

Therefore in Eq. (9) and Eq. (15), we need to replace Φ_χ^* by ζ

$$\frac{m_N}{m_N^\sigma + \delta m_N^\omega} = \zeta^{-1} = 1 - \frac{1}{3}\tilde{F}_1^\omega, \quad (40)$$

$$\frac{g_A^L + \delta g_A^L}{g_A} = \left(1 - \frac{1}{3}\zeta\tilde{F}_1^\pi\right)^{-2}, \quad (41)$$

where δg_A^L is the $1/\bar{N}$ correction to the axial coupling constant in medium.

Using Eq. (31) with the corrections included, we have

$$\zeta^{-1} = 1 + \frac{C_\omega^2 n m_N}{m_N^\sigma\left[m_N^\sigma + C_\omega^2(\Pi_{ii} + \delta\Pi_{ii})m_N^\sigma\right]}. \quad (42)$$

FIG. 4. The left graph is the higher-order correction to the ω meson propagator, the right graph is the next-to-leading order correction.

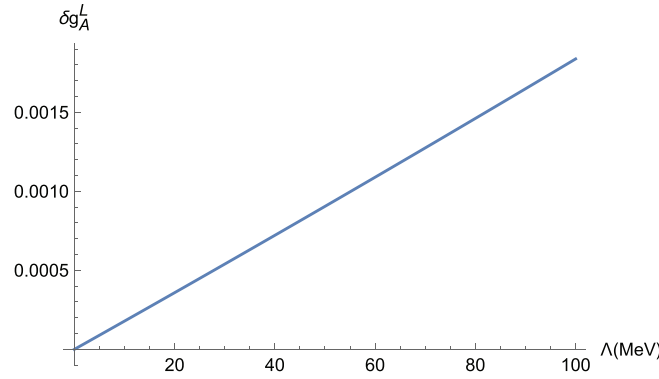

FIG. 5. Dependence of δg_A^L on the cutoff Λ.

Finally ignoring higher-order corrections to F_1^π that we argue to be ignorable, we can make an estimate of the $1/\bar{N}$ correction to g_A^L.

With the degeneracy factor $\nu = 2$ and $g_\omega = 10.15$ from Eq. (15), taking the cutoff on top of the Fermi surface to be $\Lambda \approx 10$ MeV for illustration, we obtain with (37)

$$\delta g_A^L = 1.8 \times 10^{-4} \text{ at } n = n_0 \simeq 0.16\,\text{fm}^{-3}. \quad (43)$$

The correction is extremely small. One can see roughly how it comes about as follows: The denominator in the integral of Eq. (37) in the range $m_\omega^{*2} - 1.3m_\omega^{*2}$ giving the integrand $\sim k^4/m_\omega^{*2}m_N^{\sigma 2}$ comes out always less than 1 in the integral region. Multiplied by the remaining factor $\Lambda g_\omega^2/32\pi^4$, $\delta\Pi_{ii}$ turns out to be a tenth of MeV^2, while $\Pi_{ii} = \nu p_F^3/6\pi^2 m_N^\sigma \approx 10^3$ MeV^2. The quantity ζ is insensitive to Π_{ii} given that the leading-order ω exchange contribution without polarization tensor [first diagram on the right-hand side of Fig. (1)] is the main contribution to the Landau parameter F_1^ω. Reflecting on the difference between ζ and Φ_χ^* and δg_A^L [Eq. (41)], the correction to g_A^L becomes of $\sim O(10^{-4})$.

The dependence of $\delta\Pi_{ii}$ on the cutoff Λ is almost linear, because the integrand in Eq. (37) contribute little when k is small. Therefore δg_A^L is almost linear in Λ as well, as seen in Fig. 5.

Now if one applies the same reasoning to the anomalous gyromagnetic ratio δg_l^i, one finds that the inclusion of $1/\bar{N}$ correction also receives small corrections $\sim O(10^{-4})$ by substituting Φ_χ^*. This would confirm that the pion contribution should also be unaffected in δg_l^i.

4. $1/\bar{N}$ correction in the $V_{\text{low k}}$-RG approach

Before closing this subsection on how nonlinear mesonic fields contribute to δg_A^L, we briefly comment on how the correction to the Fermi-liquid fixed-point (FLFP) approximation calculated in the $V_{\text{low k}}$-RG approach [20] would compare with what is obtained above. In fact the connection between $V_{\text{low k}}$ and FLFP was discussed in Ref. [25,26], where the $V_{\text{low k}}$ matrix element is used to calculate Landau parameters with a cutoff $\Lambda_{V\text{low k}} \approx 2.1\,\text{fm}^{-1}$. The chosen cutoff is where for the given nucleon potentials, phenomenological or chiral EFT, the $V_{\text{low k}}$ becomes RG invariant [27]. Notice that the $\Lambda_{V\text{low k}}$ is different from the cutoff Λ in Fig. 1 in Landau Fermi liquid.

In Ref. [28] the RG calculation for $V_{\text{low k}}$ (using, e.g., Paris potential) result showed that the β function of $V_{\text{low k}}$ approaches zero when $\Lambda_{V\text{low k}}$ is in the region $\Lambda_{V\text{low k}} \approx 2.0\,\text{fm}^{-1}$. In Ref. [29], the authors calculated the neutron matter ground-state energy E_0 by summing up the two-particle two-hole ring diagrams to all orders using the $V_{\text{low k}}$. It was found that $\xi = E_0/E_0^{\text{free}}$ (where E_0^{free} is the ground-state energy without quasiparticle interaction) has a remarkably mild dependence on the cutoff $\Lambda_{V\text{low k}}$. As shown in Fig. 6 in Ref. [29], $d\xi/d\Lambda_{V\text{low k}} \approx 10^{-4}$ (with the unit changed to MeV) is of the same magnitude as the correction to the dimensionless parameter F_1^ω in our case. Our result therefore is in agreement with the calculation in the $V_{\text{low k}}$ approach.

Now approaching the g_A problem in the formalism $V_{\text{low k}}$-RG, the Landau Fermi-liquid parameter would be the spin-isospin term carrying the Migdal interaction G_0' to which the tensor force would intervene. At any given density, the $V_{\text{low k}}$ potential becomes RG invariant roughly at the scale $\Lambda_{V\text{low k}} \approx 2.1\,\text{fm}^{-1}$ [30]. With the intricate cancellation between the pionic and ρ meson-exchange tensor forces suitably implemented with the BR scaling [31] the net tensor force becomes RG invariant in single-nucleon and many-nucleon interactions. Hence the net effective G_0' interaction will be at the Fermi-liquid fixed point [32]. It appears certain that how the effective $V_{\text{low k}}$ forces for other channels behave under RG scaling would be a very interesting topic as noted in the monopole matrix element in complex nuclei [33].

III. CONCLUDING REMARKS

In this work, we calculated $1/\bar{N}$ corrections to ω-meson propagators using the nonlinear bosonization of Fermi surface approach, and mapped the corrections to the FLFP result g_A^L at n_0. We ignored possible corrections to the pionic Fock term on the ground that its effect in the anomalous gyromagnetic ratio subject to a similar pionic correction can be safely ignored. We showed that the corrections δg_A^L are of order 10^{-4} and will tend to go to zero reaching the dilaton-limit fixed point. This result is connected with the intricate interplay mentioned above between the attraction due to the scalar excitation, i.e., dilaton, and the repulsion due to the ω excitation effective from low density to high density. The nonlinear structure of the Fermi surface in nuclear correlations does not enter into the leading-order and next-to-leading-order corrections to the ω meson propagator. This feature of the nonlinear bosonized theory (shown graphically in Appendix B 2) may be seen as a result of the unscaling of $g_{\omega\text{NN}}$ in one-loop order in Ref. [31], which is important for nuclear matter to be stable in the half-skyrmion phase.

It is highly notable that g_A^L remains more or less unaffected by density from finite nuclei to dense baryonic matter. A similar phenomenon seems to be in action in the pseudoconformal sound velocity $v_s^2/c^2 \approx 1/3$ in dense compact-star matter at $n \gtrsim 3n_0$. As suggested in Ref. [1], it could also reflect a hidden scale symmetry in action in nuclear correlations.

That g_A^L in nuclear matter is close to 1 has two important implications in physics that have not been duly recognized up to date: one in nuclear dynamics and the other in going beyond the standard model.

(i) Implication in nuclear dynamics. As for the first, the question is what g_A^L represents in what is observed in nuclear weak processes. The g_A^L as phrased in terms of Landau Fermi-liquid theory is the axial coupling constant g_A with which a quasiparticle on top of the Fermi sea makes the zero momentum and zero energy transfer Gamow-Teller transition, such that $q/\omega \to 0$, taking place in infinite nuclear matter. In real nuclear processes involving finite nuclei as discussed in Refs. [2,3], phrased in shell model, the closest to the Fermi-liquid result is the extreme single-particle shell model (ESPSM) applicable in superallowed Gamow-Teller transitions in doubly magic-shell nuclei. The heaviest nuclear system so far studied is the ^{100}Sn nucleus. It has been argued that the constant g_A^L obtained in the Fermi-liquid model can be closely mapped to what enters in the superallowed Gamow-Teller transition where a proton in the filled proton magic shell makes the transition to the lowest neutron in the empty neutron magic shell with $q/\omega \to 0$. Ideally it should involve a single unique daughter state. In reality the daughter state may not be unique. However with as small an uncertainty as in the doubly magic-shell nucleus, g_A^L should correspond closely to q times g_A where g_A is the axial coupling constant in (free-space) neutron β decay and q is the quenching factor [3]. What this means is that q should capture the full or exact nuclear correlations leading to the full quenching factor that gives the effective axial constant $g_A^{\text{eff}} \approx 1$ observed in nature. In nuclear physics, this implies that if one were to do the full calculation in the sense of Ref. [2], the axial coupling constant applicable in nuclear effective field theory defined at the chiral symmetry scale $\Lambda_\chi \approx 4\pi f_\pi \approx 1$ GeV should be the free-space value $g_A = 1.276...$ measured in neutron β decay.

(ii) Implication in beyond standard model (BSM). Secondly, $g_A^L \approx 1$ with $q \approx 0.78$ can have a big impact on the effort to go beyond the standard model by measuring $0\nu\beta\beta$ processes in nuclei. It appears that there can be a nontrivial renormalization of g_A in heavy nuclei induced by quantum anomaly [1] coming from the degrees of freedom integrated out of the chiral symmetry scale. Up to date, there has been no smoking-gun indication for a fundamental quenching of g_A in any nuclear processes, but the most recent measurement—heralded to have been improved—at RIKEN [34] in the superallowed GT transition in the doubly magic-shell nucleus ^{100}Sn, if confirmed, would indicate the basic axial-vector coupling constant g_A would undergo a quenching as big as 30–40 % reduction in all nuclear weak processes, this independent of the nuclear correlation effects associated with g_A^L. This would imply a huge reduction in the decay rate in $0\nu\beta\beta$ processes for going beyond the SM. This calls for revisiting the ^{100}Sn β-decay process, both experimentally and theoretically.

APPENDIX A: POWER COUNTING OF THE NONLINEAR BOSONIZED THEORY

The action of the nonlinear bonsonized theory coupled with mesons can be written schematically as

$$S = \int_{\boldsymbol{x},\boldsymbol{p}} dt \left\langle f, \partial_t - \omega_0 - \frac{(\boldsymbol{p}+\boldsymbol{\omega})^2}{2m_N^\sigma} \right\rangle + S_\omega, \tag{A1}$$

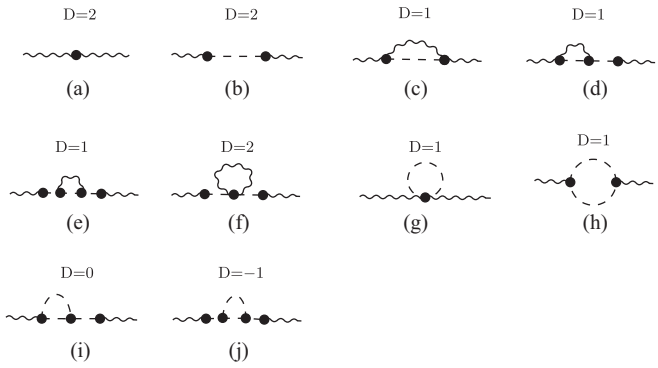

FIG. 6. Corrections to the ω meson propagator in nonlinear bosonized theory.

where

$$f = f_0 - \{\phi, f_0\} + \tfrac{1}{2}\{\phi, \{\phi, f_0\}\} - \cdots = \Theta(p_F - |\boldsymbol{p}|) + \delta(|\boldsymbol{p}| - p_F)\boldsymbol{n}_\theta \cdot \nabla_x \phi + \cdots . \tag{A2}$$

The fermion density is

$$n(t,\boldsymbol{x}) = \nu \int_{\boldsymbol{p}} f = \frac{\nu p_F^3}{6\pi^2} + \frac{\nu p_F^2}{(2\pi)^3}\int d^2\theta \boldsymbol{n}_\theta \cdot \nabla\phi(t,\boldsymbol{x},\theta) + \cdots . \tag{A3}$$

In the action expanded in terms of ϕ, the free propagator of ϕ comes out

$$\langle\phi\phi'\rangle(q_0,\boldsymbol{q}) = i\frac{(2\pi)^3}{p_F^2}\frac{\delta^2(\theta-\theta')}{\boldsymbol{n}_\theta\cdot\boldsymbol{q}\left(q_0 - \frac{p_F}{m_N^\sigma}\boldsymbol{n}_\theta\cdot\boldsymbol{q} + i\epsilon\right)}. \tag{A4}$$

The details are relegated to Ref. [5].

The density operator n has mass dimension 3. The mass dimension as well as the scaling dimension of the bosonic degrees of freedom $\phi(t,\boldsymbol{x},\theta)$ is zero. Note that ϕ always comes with one ∇_x/p_F.

Let us count how many times p_F appears. Figure 6(a) has a vertex coming from Eq. (A1) $\sim p_F^3/m_N^\sigma$, with $m_N^\sigma \sim p_F$ at n_0, Fig. 6(a) is $\sim p_F^2$. Figure 6(b) has two vertexes $\sim p_F^3/m_N^\sigma$ and a internal ϕ line $\sim p_F^{-2}$, so Fig. 6(b) is $\sim p_F^2$.

For loop diagrams in the bosonic theory, every internal ω meson line contributes p_F^{-2} because $m_\omega^* \sim p_F$. Every loop integral contributes p_F^4. Figure 6(c) has two vertices $\sim p_F^2/m_N^\sigma$, a loop $\sim p_F^4$, two internal lines $\sim p_F^{-2}$. There is a caveat here as will be elaborated in Fig. 7; a ϕ line carrying large momentum $\boldsymbol{k}$ is suppressed by a factor Λ/p_F [8]. So Fig. 6(c) is $\sim p_F$.

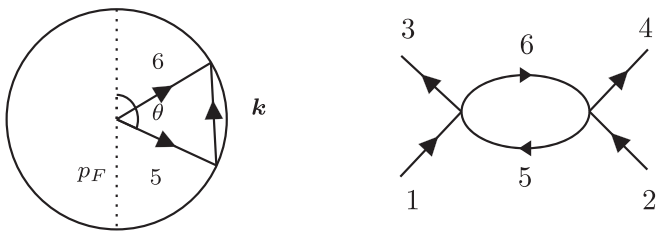

FIG. 7. The phase space restriction when momentum transfer $\boldsymbol{k}$ is large.

Other diagrams are shown in Fig. 6, with Fig. 6(d) meaning the diagram is $\sim p_F^D$.

The Figs. 6(a)–6(b) are the leading-order corrections to the free ω meson propagator. There are many diagrams in the next-to the leading orders. However, most diagrams do not contribute in the limit that the external momentum $\boldsymbol{q}/q_0 \to 0$. The next-to-leading-order contributions to the meson propagator should be the $D = 1$ diagrams, which contain Figs. 6(c), 6(d) 6(e), 6(g), 6(h). This power counting is valid for one-loop graphs. For higher loop diagrams, however, there are more suppressions coming from phase space arguments with which we are not concerned in this work.

APPENDIX B: CORRECTIONS TO THE ω MESON PROPAGATOR

1. Leading-order corrections

Amputating the ω line, Fig. 6(a) is simply n/m_N^σ with $n = \nu p_F^3/6\pi^2$. And the Fig. 6(b) is given by

$$\begin{aligned}(B) &= -i\frac{p_F^4}{(2\pi)^6}\int\frac{d\boldsymbol{p}}{(2\pi)^3}\delta(|\boldsymbol{p}|-p_F)\boldsymbol{n}_\theta \cdot i\boldsymbol{q}\int\frac{d\boldsymbol{p}'}{(2\pi)^3}\delta(|\boldsymbol{p}'|-p_F)\boldsymbol{n}'_\theta\cdot i(-\boldsymbol{q})\langle\phi\phi'\rangle\frac{\boldsymbol{p}\cdot\boldsymbol{p}'}{m_N^{\sigma 2}}\\ &= \frac{p_F^2}{(2\pi)^3}\frac{\nu p_F^2}{3m_N^{\sigma 2}}\int d^2\theta\frac{\boldsymbol{n}_\theta\cdot\boldsymbol{q}}{q_0 - \frac{p_F}{m_N^\sigma}\boldsymbol{n}_\theta\cdot\boldsymbol{q}}\\ &= -\frac{\nu p_F^3}{6\pi^2 m_N^\sigma}\left(1 + \frac{m_N^\sigma|q_0|}{2p_F|\boldsymbol{q}|}\log\frac{m_N^\sigma|q_0| - p_F|\boldsymbol{q}|}{m_N^\sigma|q_0| + p_F|\boldsymbol{q}|}\right),\end{aligned} \tag{B1}$$

where $q_\mu = (q_0,\boldsymbol{q})$ is external momentum. The sum of Fig. 6(a) and 6(b) reproduces Eq. (36).

2. Next-to-leading-order corrections

To calculate in Fig. 6(c), we have to divide the loop momentum into two parts, one from 0 to Λ, denoted as part I, and the other from Λ to $2p_F$, denoted as part II. While the part I is not suppressed by phase space argument, the part II is suppressed by a factor Λ/p_F [8]. However, the part I is suppressed by $(\Lambda/p_F)^3$ compared to the part II due to the integration region, so the region II should give the dominant contribution

$$(C) = \int_{II}\frac{d^3\boldsymbol{k}dk_0}{(2\pi)^4}\frac{1}{m_N^{\sigma 2}}\frac{-ig_\omega^2}{(q_\mu - k_\mu)^2 - m_\omega^{*2} + i\epsilon}\frac{\nu p_F^2}{2(2\pi)^3} \times\int d^2\theta\frac{\boldsymbol{n}_\theta\cdot\boldsymbol{k}}{k_0 - \frac{p_F}{m_N^\sigma}\boldsymbol{n_\theta}\cdot\boldsymbol{k} + i\epsilon}, \tag{B2}$$

where $k_\mu = (k_0,\boldsymbol{k})$ is the loop momentum. The reason why the part II is suppressed by Λ/p_F is shown in Fig. 7, given in the fermionic description

When we take $\Lambda \to 0$, then all fermions 1-6 lie at the Fermi surface. Suppose the difference between $\boldsymbol{k_3}$ and $\boldsymbol{k_1}$ is $\boldsymbol{k}$. When the momentum transfer $|\boldsymbol{k}|$ is within Λ, i.e., $|\boldsymbol{k}| \to 0$, the loop momentum $\boldsymbol{k_5}$ runs freely at the Fermi surface. However, when $\boldsymbol{k}$ is large like the one in Fig. 7, $\boldsymbol{k_5}$ is restricted

in a specific point at the Fermi surface corresponding to the polar angle θ. When Λ is not exactly zero, the specific point will expand to a region of angle Λ/p_F. This argument is made in two dimensions. In three dimensions, there is an extra azimuthal angle that allows the fermions 5 and 6 to run freely.

In the bosonic theory, the second integral in Eq. (B2) is easy to work out. When the angle θ is in a fixed region rather than the whole Fermi surface, the integrand is a quantity dependent of $|\boldsymbol{k}|$ and independent of angle. The integral will be replaced by the integrand times the angle region. After some manipulation, $\boldsymbol{n}_\theta \cdot \boldsymbol{k} = -\boldsymbol{k}^2/2p_F$. So Fig. 6(c) becomes

$$
\begin{aligned}
(C) &= i\frac{\nu\Lambda p_F}{2(2\pi)^2 m_N^{\sigma 2}}\int_{II}\frac{d\boldsymbol{k}dk_0}{(2\pi)^4}\frac{g_\omega^2}{(q_\mu-k_\mu)^2-m_\omega^{*2}+i\epsilon}\frac{\frac{\boldsymbol{k}^2}{2p_F}}{k_0+\frac{\boldsymbol{k}^2}{2m_N^\sigma}+i\epsilon}\\
&= i\frac{\nu\Lambda g_\omega^2}{16\pi^2 m_N^{\sigma 2}}\int_{II}\frac{d\boldsymbol{k}dk_0}{(2\pi)^4}\frac{\boldsymbol{k}^2}{\left[k_0-\left(q_0+\sqrt{(\boldsymbol{q}-\boldsymbol{k})^2+m_\omega^{*2}}\right)+i\epsilon\right]\left[k_0-\left(q_0-\sqrt{(\boldsymbol{q}-\boldsymbol{k})^2+m_\omega^{*2}}\right)-i\epsilon\right]\left(k_0+\frac{\boldsymbol{k}^2}{2m_N^\sigma}+i\epsilon\right)}\\
&= -\frac{\nu\Lambda g_\omega^2}{64\pi^4 m_N^{\sigma 2}}\int_\Lambda^{2p_F}dk\frac{k^4}{k^2+m_\omega^{*2}-\frac{k^2\sqrt{k^2+m_\omega^{*2}}}{2m_N^\sigma}}.
\end{aligned}
\tag{B3}
$$

The nonlinear bosonized theory has some similarity to nonlinear σ model. For this reason, Figs. 6(d)–6(f) vanish in the limit the momentum transfer goes to zero. It can be shown that Figs. 6(g) and 6(h) also vanish in the limit. Therefore Fig. 6(c) is the only diagram that needs to be calculated.

In the limit $|\boldsymbol{q}|/q_0 \to 0, q_0 \to 0$, the nonlinear structure of the Fermi surface does not affect the next-leading-order corrections to the ω meson propagator because Fig. 6(c) does not contain the vertex that connects two dashed lines. The Figs. 6(d) and 6(e) can actually be seen as loop corrections to the ϕ-ω vertex. If not amputated, the ϕ-ω vertex in the nonlinear bosonized theory corresponds to the ω-N-N vertex in Ref. [31]. So Figs. 6(d) and 6(e) vanishing in the limit $|\boldsymbol{q}|/q_0 \to 0$ should be seen as a result of unscaling of $g_{\omega\mathrm{NN}}$ in one fermion-loop order.

[1] M. Rho, Anomaly-induced quenching of g_A in nuclear matter and impact on search for neutrinoless $\beta\beta$ decay, Symmetry **15**, 1648 (2023).

[2] D. H. Wilkinson, Renormalization of the axial-vector coupling constant in nuclear beta decay, Phys. Rev. C **7**, 930 (1973).

[3] J. T. Suhonen, Value of the axial-vector coupling strength in β and $\beta\beta$ decays: A review, Front. Phys. **5**, 55 (2017); J. Engel and J. Menèndez, Status and future of nuclear matrix elements for neutrinoless double-beta decay: A review, Rep. Prog. Phys. **80**, 046301 (2017).

[4] G. B. King, L. Andreoli, S. Pastore, M. Piarulli, R. Schiavilla, R. B. Wiringa, J. Carlson, and S. Gandolfi, Chiral effective field theory calculations of weak transitions in light nuclei, Phys. Rev. C **102**, 025501 (2020).

[5] L. V. Delacretaz, Y.-H. Du, U. Mehta, and D. T. Son, Nonlinear bosonization of Fermi surfaces: The method of coadjoint orbits, Phys. Rev. Res. **4**, 033131 (2022).

[6] G. E. Brown and M. Rho, Scaling effective Lagrangians in a dense medium, Phys. Rev. Lett. **66**, 2720 (1991).

[7] T. Appelquist, J. Ingoldby, and M. Piai, Dilaton effective field theory, Universe **9**, 10 (2023).

[8] R. Shankar, Renormalization group approach to interacting fermions, Rev. Mod. Phys. **66**, 129 (1994).

[9] J. Polchinski, Effective field theory and the Fermi surface, arXiv:hep-th/9210046.

[10] B. Friman and M. Rho, From chiral Lagrangians to Landau Fermi liquid theory of nuclear matter, Nucl. Phys. A **606**, 303 (1996).

[11] R. J. Crewther, Genuine dilatons in gauge theories, Universe **6**, 96 (2020).

[12] R. J. Crewther and L. C. Tunstall, Status of chiral-scale perturbation theory, PoS **CD15**, 132 (2015), arXiv:1510.01322.

[13] S. R. Beane and U. van Kolck, The dilated chiral quark model, Phys. Lett. B **328**, 137 (1994).

[14] M. Bando, T. Kugo, S. Uehara, K. Yamawaki, and T. Yanagida, Is ρ meson a dynamical gauge boson of hidden local symmetry? Phys. Rev. Lett. **54**, 1215 (1985).

[15] M. Harada and K. Yamawaki, Hidden local symmetry at loop: A new perspective of composite gauge boson and chiral phase transition, Phys. Rep. **381**, 1 (2003).

[16] M. Rho and Y. L. Ma, Manifestation of hidden symmetries in baryonic matter: From finite nuclei to neutron stars, Mod. Phys. Lett. A **36**, 2130012 (2021).

[17] Y. L. Ma and M. Rho, Towards the hadron–quark continuity via a topology change in compact stars, Prog. Part. Nucl. Phys. **113**, 103791 (2020).

[18] J. D. Walecka, A Theory of highly condensed matter, Ann. Phys. **83**, 491 (1974).

[19] G. E. Brown and M. Rho, Velocity dependence of the nucleon-nucleon interaction, exchange currents and enhancement of the dipole sum-rule in nuclei, Nucl. Phys. A **338**, 269 (1980).

[20] W. G. Paeng, T. T. S. Kuo, H. K. Lee, Y. L. Ma, and M. Rho, Scale-invariant hidden local symmetry, topology change, and dense baryonic matter. II, Phys. Rev. D **96**, 014031 (2017).

[21] C. Song, Dense nuclear matter: Landau Fermi liquid theory and chiral Lagrangian with scaling, Phys. Rep. **347**, 289 (2001).

[22] A. B. Migdal, *Theory of Finite Fermi Systems and Application to Finite Nuclei* (Interscience, London, 1967).
[23] R. Nolte, A. Baumann, K. W. Rose, and M. Schumacher, Effect of exchange currents in E1 sum rule and orbital g-factor in ^{209}Bi, Phys. Lett. B **173**, 388 (1986).
[24] T. Matsui, Fermi liquid properties of nuclear matter in a relativistic mean - field theory, Nucl. Phys. A **370**, 365 (1981).
[25] A. Schwenk, G. E. Brown, and B. Friman, Low momentum nucleon-nucleon interaction and Fermi liquid theory, Nucl. Phys. A **703**, 745 (2002).
[26] J. W. Holt, G. E. Brown, J. D. Holt, and T. T. S. Kuo, Nuclear matter with Brown-Rho-scaled Fermi liquid interactions, Nucl. Phys. A **785**, 322 (2007).
[27] S. K. Bogner, T. T. S. Kuo, A. Schwenk, D. R. Entem, and R. Machleidt, Towards a model independent low momentum nucleon nucleon interaction, Phys. Lett. B **576**, 265 (2003).
[28] S. K. Bogner, A. Schwenk, T. T. S. Kuo, and G. E. Brown, Renormalization group equation for low momentum effective nuclear interactions, arXiv:nucl-th/0111042.
[29] L. W. Siu, T. T. S. Kuo, and R. Machleidt, Low-momentum ring diagrams of neutron matter at and near the unitary limit, Phys. Rev. C **77**, 034001 (2008).
[30] M. Rho, In search of a pristine signal for (scale-)chiral symmetry in nuclei, Int. J. Mod. Phys. E **26**, 1740023 (2017).
[31] W.-G. Paeng, H. K. Lee, M. Rho, and C. Sasaki, Interplay between ω-nucleon interaction and nucleon mass in dense baryonic matter, Phys. Rev. D **88**, 105019 (2013).
[32] M. Rho and L. Q. Shao, $V_{\rm lowk}$ Renormalization group flow, vector manifestation and sound velocity in massive compact stars, arXiv:2402.00755 [nucl-th].
[33] N. Tsunoda, T. Otsuka, K. Tsukiyama, and M. Hjorth-Jensen, Renormalization persistency of tensor force in nuclei, Phys. Rev. C **84**, 044322 (2011).
[34] D. Lubos *et al.*, Improved value for the Gamow-Teller strength of the ^{100}Sn beta decay, Phys. Rev. Lett. **122**, 222502 (2019).